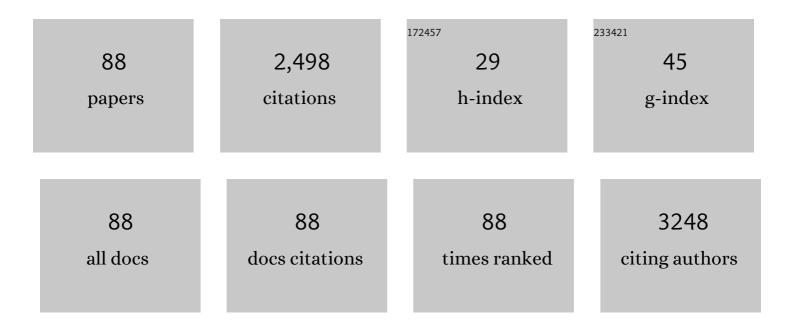
List of Publications by Year in descending order

Source: https://exaly.com/author-pdf/6581374/publications.pdf Version: 2024-02-01



#	Article	IF	CITATIONS
1	Degradation of polyvinyl chloride microplastics via an electro-Fenton-like system with a TiO2/graphite cathode. Journal of Hazardous Materials, 2020, 399, 123023.	12.4	194
2	The Secreted Peptide PIP1 Amplifies Immunity through Receptor-Like Kinase 7. PLoS Pathogens, 2014, 10, e1004331.	4.7	186
3	A Wheat <i>SIMILAR TO RCD-ONE</i> Gene Enhances Seedling Growth and Abiotic Stress Resistance by Modulating Redox Homeostasis and Maintaining Genomic Integrity Â. Plant Cell, 2014, 26, 164-180.	6.6	113
4	Constructing Cuâ^'C Bonds in a Graphdiyneâ€Regulated Cu Singleâ€Atom Electrocatalyst for CO ₂ Reduction to CH ₄ . Angewandte Chemie - International Edition, 2022, 61, .	13.8	92
5	Unraveling a Single-Step Simultaneous Two-Electron Transfer Process from Semiconductor to Molecular Catalyst in a CoPy/CdS Hybrid System for Photocatalytic H ₂ Evolution under Strong Alkaline Conditions. Journal of the American Chemical Society, 2016, 138, 10726-10729.	13.7	79
6	THI1, a Thiamine Thiazole Synthase, Interacts with Ca2+-Dependent Protein Kinase CPK33 and Modulates the S-Type Anion Channels and Stomatal Closure in Arabidopsis Â. Plant Physiology, 2016, 170, 1090-1104.	4.8	73
7	NRGA1, a Putative Mitochondrial Pyruvate Carrier, Mediates ABA Regulation of Guard Cell Ion Channels and Drought Stress Responses in Arabidopsis. Molecular Plant, 2014, 7, 1508-1521.	8.3	65
8	The use of phosphonates for constructing 3d–4f clusters at high oxidation states: synthesis and characterization of two unusual heterometallic CeMn complexes. Dalton Transactions, 2010, 39, 7276.	3.3	57
9	Overexpression of wheat NF-YA10 gene regulates the salinity stress response in Arabidopsis thaliana. Plant Physiology and Biochemistry, 2015, 86, 34-43.	5.8	57
10	CYCLIN-DEPENDENT KINASE G2 regulates salinity stress response and salt mediated flowering in Arabidopsis thaliana. Plant Molecular Biology, 2015, 88, 287-299.	3.9	53
11	Autophagy: Multiple Mechanisms to Protect Skin from Ultraviolet Radiation-Driven Photoaging. Oxidative Medicine and Cellular Longevity, 2019, 2019, 1-14.	4.0	53
12	Molecular and Electronic Structures of Six-Coordinate "Low-Valent― [M(^{Me} bpy) ₃] ⁰ (M = Ti, V, Cr, Mo) and [M(tpy) ₂] ⁰ (M = Ti, V, Cr), and Seven-Coordinate [MoF(^{Me} bpy) ₃](PF ₆) and [MX(tpy) ₂](PF ₆) (M = Mo, X = Cl and M = W, X = F). Inorganic Chemistry, 2013, 52, 12763-12776.	4.0	52
13	A wheat aminocyclopropane-1-carboxylate oxidase gene, TaACO1, negatively regulates salinity stress in Arabidopsis thaliana. Plant Cell Reports, 2014, 33, 1815-1827.	5.6	51
14	Mitochondrial Pyruvate Carriers Prevent Cadmium Toxicity by Sustaining the TCA Cycle and Glutathione Synthesis. Plant Physiology, 2019, 180, 198-211.	4.8	51
15	Effects of straw return with N fertilizer reduction on crop yield, plant diseases and pests and posts and potential heavy metal risk in a Chinese rice paddy: A field study of 2 consecutive wheat-rice cycles. Environmental Pollution, 2021, 288, 117741.	7.5	51
16	Arabidopsis thaliana calmodulin-like protein CML24 regulates pollen tube growth by modulating the actin cytoskeleton and controlling the cytosolic Ca2+ concentration. Plant Molecular Biology, 2014, 86, 225-236.	3.9	48
17	<i>In situ</i> construction of graphdiyne/CuS heterostructures for efficient hydrogen evolution reaction. Materials Chemistry Frontiers, 2019, 3, 821-828.	5.9	47
18	<scp><i>A</i></scp> <i>rabidopsis thaliana</i> â€ <scp>CML</scp> 25 mediates the <scp><scp>Ca²⁺</scp></scp> regulation of <scp><scp>K⁺</scp> transmembrane trafficking during pollen germination and tube elongation. Plant, Cell and Environment, 2015, 38, 2372-2386.</scp>	5.7	46

#	Article	IF	CITATIONS
19	Molecular and Electronic Structures of the Members of the Electron Transfer Series [Mn(bpy) ₃] ^{<i>n</i>} (<i>n</i> = 2+, 1+, 0, 1â^') and [Mn(tpy) ₂] ^{<i>m</i>} (<i>m</i> = 4+, 3+, 2+, 1+, 0). An Experimental and Density Functional Theory Study. Inorganic Chemistry, 2014, 53, 2276-2287.	4.0	45
20	CoS2 nanowires supported graphdiyne for highly efficient hydrogen evolution reaction. Journal of Energy Chemistry, 2021, 60, 272-278.	12.9	44
21	ZmOST1 mediates abscisic acid regulation of guard cell ion channels and drought stress responses. Journal of Integrative Plant Biology, 2019, 61, 478-491.	8.5	43
22	Stabilization of cobalt clusters with graphdiyne enabling efficient overall water splitting. Nano Energy, 2020, 74, 104852.	16.0	43
23	Synthesis and Characterization of a Family of Penta- and Tetra-Manganese(III) Complexes Derived from an Assembly System Containing <i>tert</i> -Butylphosphonic Acid. Inorganic Chemistry, 2008, 47, 5580-5590.	4.0	42
24	UVA Irradiation Enhances Brusatol-Mediated Inhibition of Melanoma Growth by Downregulation of the Nrf2-Mediated Antioxidant Response. Oxidative Medicine and Cellular Longevity, 2018, 2018, 1-15.	4.0	35
25	Wheat NF-YA10 functions independently in salinity and drought stress. Bioengineered, 2015, 6, 245-247.	3.2	33
26	Synthesis and characterization of nona- and trideca-nuclear manganese phosphonate clusters. Dalton Transactions, 2008, , 4612.	3.3	32
27	A trimanganese cluster-based 2D layer framework with facile single-crystal-to-single-crystal transformation to afford a 1D chain structure. CrystEngComm, 2010, 12, 1467.	2.6	32
28	Fluorine in the environment in an endemic fluorosis area in Southwest, China. Environmental Research, 2020, 184, 109300.	7.5	32
29	Synthesis and characterization of a series of manganese phosphonate complexes with various valences and nuclearity. Dalton Transactions, 2009, , 994-1003.	3.3	31
30	The LRR-RLK Protein HSL3 Regulates Stomatal Closure and the Drought Stress Response by Modulating Hydrogen Peroxide Homeostasis. Frontiers in Plant Science, 2020, 11, 548034.	3.6	30
31	Six Co(II) Coordination Polymers Based on Two Isomeric Semirigid Ether-Linked Aromatic Tetracarboxylate Acid: Syntheses, Structural Comparison, and Magnetic Properties. Crystal Growth and Design, 2017, 17, 5533-5543.	3.0	29
32	Mitochondrial pyruvate carrier 1 mediates abscisic acid-regulated stomatal closure and the drought response by affecting cellular pyruvate content in Arabidopsis thaliana. BMC Plant Biology, 2017, 17, 217.	3.6	28
33	Microwave-assisted liquefaction of carbohydrates for 5-hydroxymethylfurfural using tungstophosphoric acid encapsulated dendritic fibrous mesoporous silica as a catalyst. Science of the Total Environment, 2021, 760, 143379.	8.0	28
34	Structural and Spectroscopic Characterization of Rhenium Complexes Containing Neutral, Monoanionic, and Dianionic Ligands of 2,2′-Bipyridines and 2,2′:6,2″-Terpyridines: An Experimental and Density Functional Theory (DFT)-Computational Study. Inorganic Chemistry, 2016, 55, 5019-5036.	4.0	26
35	Two tetranuclear 3d–4f heterometal complexes Mn ₂ Ln ₂ (Ln = Dy, Gd): synthesis, structure, magnetism, and electrocatalytic reactivity for water oxidation. New Journal of Chemistry, 2018, 42, 5798-5805.	2.8	26
36	Discovery of DNA Topoisomerase I Inhibitors with Low-Cytotoxicity Based on Virtual Screening from Natural Products. Marine Drugs, 2017, 15, 217.	4.6	25

#	Article	IF	CITATIONS
37	OXS2 is Required for Salt Tolerance Mainly through Associating with Salt Inducible Genes, CA1 and Araport11, in Arabidopsis. Scientific Reports, 2019, 9, 20341.	3.3	24
38	The effect of torrefaction and ZSM-5 catalyst for hydrocarbon rich bio-oil production from co-pyrolysis of cellulose and low density polyethylene via microwave-assisted heating. Science of the Total Environment, 2021, 754, 142174.	8.0	24
39	Synthesis and characterization of a family of tetranuclear manganese(iii) phosphonate complexes. New Journal of Chemistry, 2007, 31, 2103.	2.8	22
40	Physiological and Molecular Processes Associated with Long Duration of ABA Treatment. Frontiers in Plant Science, 2018, 9, 176.	3.6	22
41	Telomerase reverse transcriptase mediates EMT through NF-κB signaling in tongue squamous cell carcinoma. Oncotarget, 2017, 8, 85492-85503.	1.8	21
42	Two Trinuclear Cu ^{II} Complexes: Effect of Phosphonate Ligand on the Magnetic Property and Electrocatalytic Reactivity for Water Oxidation. Chemistry - an Asian Journal, 2019, 14, 2685-2693.	3.3	20
43	Naphthalenones and Depsidones from a Sponge-Derived Strain of the Fungus Corynespora cassiicola. Molecules, 2016, 21, 160.	3.8	19
44	ALA_PDT Promotes Ferroptosis-Like Death of Mycobacterium abscessus and Antibiotic Sterilization via Oxidative Stress. Antioxidants, 2022, 11, 546.	5.1	18
45	Determining the Electronic Structure of a Series of [(phen) ₃ M] ⁰ (M = Ti, V,) Tj ETQq1 Ligands vs. Ï€â€Radical Anions. European Journal of Inorganic Chemistry, 2015, 2015, 3246-3254.	1 0.7843 2.0	14 rgBT /Ove 16
46	Spatial variation and fractionation of fluoride in tobacco-planted soils and leaf fluoride concentration in tobacco in Bijie City, Southwest China. Environmental Science and Pollution Research, 2021, 28, 26112-26123.	5.3	15
47	Competitive immobilization of Pb in an aqueous ternary-metals system by soluble phosphates with varying pH. Chemosphere, 2016, 159, 58-65.	8.2	14
48	Electrocatalytic water oxidation studies of a tetranuclear Cu(<scp>ii</scp>) complex with cubane-like core Cu ₄ (μ ₃ -O) ₄ . New Journal of Chemistry, 2019, 43, 4640-4647.	2.8	14
49	A ras-related small GTP-binding protein, RabE1c, regulates stomatal movements and drought stress responses by mediating the interaction with ABA receptors. Plant Science, 2021, 306, 110858.	3.6	14
50	Reproductive toxicity and underlying mechanisms of di(2-ethylhexyl) phthalate in nematode Caenorhabditis elegans. Journal of Environmental Sciences, 2021, 105, 1-10.	6.1	14
51	Characterization and analysis of DLC films with different thickness deposited by RF magnetron PECVD. Rare Metals, 2012, 31, 198-203.	7.1	13
52	Effects of low-dose ALA-PDT on fibroblast photoaging induced by UVA irradiation and the underlying mechanisms. Photodiagnosis and Photodynamic Therapy, 2019, 27, 79-84.	2.6	13
53	Secreted Peptide PIP1 Induces Stomatal Closure by Activation of Guard Cell Anion Channels in Arabidopsis. Frontiers in Plant Science, 2020, 11, 1029.	3.6	13
54	Associations between Serum-Intact Parathyroid Hormone, Serum 25-Hydroxyvitamin D. Oral Vitamin D Analogs and Metabolic Syndrome in Peritoneal Dialysis Patients: A Multi-Center Cross-Sectional Study. Peritoneal Dialysis International, 2014, 34, 447-455.	2.3	12

#	Article	IF	CITATIONS
55	Soil fungal communities affect the chemical quality of flue-cured tobacco leaves in Bijie, Southwest China. Scientific Reports, 2022, 12, 2815.	3.3	12
56	The ongoing story: the mitochondria pyruvate carrier 1 in plant stress response in Arabidopsis. Plant Signaling and Behavior, 2014, 9, e973810.	2.4	11
57	Two novel Co (II) oordination polymers as bifunctional materials for efficient photocatalytic degradation of dyes and electrocatalytic water oxidation. Applied Organometallic Chemistry, 2020, 34, e5767.	3.5	11
58	The Cyclophilin ROC3 Regulates ABA-Induced Stomatal Closure and the Drought Stress Response of Arabidopsis thaliana. Frontiers in Plant Science, 2021, 12, 668792.	3.6	11
59	Stabilization of Cu/Ni Alloy Nanoparticles with Graphdiyne Enabling Efficient CO2 Reduction. Chemical Research in Chinese Universities, 2021, 37, 1328-1333.	2.6	11
60	<scp>TaSRO1</scp> plays a dual role in suppressing <scp>TaSIP1</scp> to fine tune mitochondrial retrograde signalling and enhance salinity stress tolerance. New Phytologist, 2022, 236, 495-511.	7.3	11
61	Antibacterial Δ ¹ â€3â€Ketosteroids from the South China Sea Gorgonian Coral <i>Subergorgia rubra</i> . Chemistry and Biodiversity, 2015, 12, 1068-1074.	2.1	10
62	Recent advances of graphdiyne: synthesis, functionalization, and electrocatalytic applications. Materials Chemistry Frontiers, 2021, 5, 7964-7981.	5.9	9
63	A novel wheat cysteine-rich receptor-like kinase gene CRK41 is involved in the regulation of seed germination under osmotic stress in Arabidopsis thaliana. Journal of Plant Biology, 2017, 60, 571-581.	2.1	8
64	Coordination Modes, Oxidation, and Protonation Levels of 2,6-Pyridinediimine and 2,2′:6′,2′̕Terpyridine Ligands in New Complexes of Cobalt, Zirconium, and Ruthenium. An Experimental and Density Functional Theory Computational Study. Inorganic Chemistry, 2019, 58, 121-132.	4.0	8
65	UV-responsive AKBA@ZnO nanoparticles potential for polymorphous light eruption protection and therapy. Materials Science and Engineering C, 2020, 107, 110254.	7.3	8
66	Two biologically inspired tetranuclear nickel(II) catalysts: effect of the geometry of Ni4 core on electrocatalytic water oxidation. Journal of Biological Inorganic Chemistry, 2021, 26, 205-216.	2.6	8
67	<scp>SORTING NEXIN2</scp> proteins mediate stomatal movement and the response to drought stress by modulating trafficking and protein levels of the <scp>ABA</scp> exporter <scp>ABCG25</scp> . Plant Journal, 2022, 110, 1603-1618.	5.7	8
68	Constructing Cuâ^'C Bonds in a Graphdiyneâ€Regulated Cu Singleâ€Atom Electrocatalyst for CO ₂ Reduction to CH ₄ . Angewandte Chemie, 2022, 134, .	2.0	8
69	Synthesis and characterization of two manganese tert-butylphosphonate complexes. Journal of Molecular Structure, 2009, 920, 242-247.	3.6	7
70	Low-level PDT treatment modulated photoaging mediated by UVA irradiation through regulating Bach2. Photodiagnosis and Photodynamic Therapy, 2020, 29, 101606.	2.6	7
71	Graphdiyne‣tabilized Silver Nanoparticles as an Efficient Electrocatalyst for CO 2 Reduction. Advanced Energy and Sustainability Research, 2021, 2, 2100037.	5.8	7
72	Effect of PDI ligand binding pattern on the electrocatalytic activity of two Ru(II) complexes for CO 2 reduction. Applied Organometallic Chemistry, 2020, 34, e5551.	3.5	6

#	Article	IF	CITATIONS
73	Five novel MOFs with various dimensions as efficient catalysts for oxygen evolution reactions. CrystEngComm, 2021, 23, 5475-5480.	2.6	6
74	Simultaneous removal of Cr and organic matters via coupling Cr-Fenton-like reaction with Cr flocculation: The key role of Cr flocs on coupling effect. Chemosphere, 2022, 287, 131991.	8.2	6
75	Preparation of H-terminated and aminated diamond like carbon surfaces. Rare Metals, 2012, 31, 189-192.	7.1	5
76	Electrocatalytic CO2 Reduction and H2 Evolution by a Copper (II) Complex with Redox-Active Ligand. Molecules, 2022, 27, 1399.	3.8	5
77	The Electron Transfer Series [MoIII(bpy)3]n(n=3+, 2+, 1+, 0, 1â^'), and the Dinuclear Species [{MoIIICl(Mebpy)2}2(μ2-O)]Cl2and [{MoIV(tpy.)2}2(μ2-MoO4)](PF6)2â‹4 MeCN. Chemistry - A Europe 2014, 20, n/a-n/a.	ea s, ournal	, 4
78	Cembranoid Diterpenes from the South China Sea Soft Coral Sinularia compacta. Chemistry of Natural Compounds, 2017, 53, 181-184.	0.8	4
79	A mononuclear copper complex as bifunctional electrocatalyst for CO2 reduction and water oxidation. Journal of Electroanalytical Chemistry, 2021, 886, 115106.	3.8	4
80	Bioinspired cobalt molecular electrocatalyst for water oxidation coupled with carbon dioxide reduction. Applied Organometallic Chemistry, 2021, 35, e6371.	3.5	4
81	Study of the size-dependent properties of ScnAl (n= 1–14) clusters by density-functional theory. Journal of Physics Condensed Matter, 2009, 21, 046004.	1.8	3
82	A type of voltage-dependent Ca2+ channel on Vicia faba guard cell plasma membrane outwardly permeates K+. Protoplasma, 2012, 249, 699-708.	2.1	3
83	Clicking cyclophane to boron doped diamond surfaces. Science Bulletin, 2013, 58, 2898-2902.	1.7	3
84	Synthesis and electrocatalytic reactivity for water oxidation of two ceriumÂcomplexes. Journal of Coordination Chemistry, 2018, 71, 1415-1429.	2.2	3
85	Catalytic Oxidation of Trichloroethylene over RuO2 Supported on Ceria-zirconia Mixed Oxide. Chemical Research in Chinese Universities, 2019, 35, 71-78.	2.6	3
86	Fluorine in 20 vegetable species and 25 lettuce cultivars grown on a contaminated field adjacent to a brick kiln. Environmental Geochemistry and Health, 2023, 45, 1655-1667.	3.4	3
87	Clicking ferrocene to halogenated boron-doped diamond surfaces. Rare Metals, 2013, 32, 100-104.	7.1	1
88	Turbo Equalization Performance Analysis and Application in the HF Communication System. , 2017, , .		0